Geomechanics and Engineering, *Vol. 43, No. 3 (2025) 243-257*
https://doi.org/10.12989/gae.2025.43.3.243

Evaluation of kinematic bending moment for seismically loaded piles at the interface in layered ground

Ruping Luo[1,2,3a], Jie Li[2b], Bitang Zhu*[1,2,3] and Xuehui Jiang[2c]

[1]*State Key Laboratory of Safety and Resilience of Civil Engineering in Mountain Area, East China Jiaotong University, Nanchang, 330013, P.R. China*
[2]*School of Civil Engineering and Architecture, East China Jiaotong University, Nanchang 330013, P.R. China*
[3]*Engineering Research & Development Centre for Underground Technology of Jiangxi Province; East China Jiaotong University, Nanchang 330013, P.R. China*

(*Received November 30, 2023, Revised August 24, 2025, Accepted October 14, 2025*)

Abstract. The importance of the kinematic effects, especially at the interface in the layered ground, on the behavior of seismically loaded piles, has been recognized well by academia and industry. In this paper, several widely utilized simplified models for estimating the maximum kinematic pile bending at the interfaces in the layered ground are reviewed, and a series of three-dimensional (3D) numerical models for piles with various spacings, pile numbers, ground conditions, and pile dimensions are employed to examine the kinematic interactions between soil and pile foundations. Based on the extensive numerical parametric study, the group reduction effects for kinematic bending moment are discussed, and the feasibility and reliability of the reviewed simplified models under different ground conditions are evaluated sufficiently. Finally, several empirical formulas for estimating the maximum kinematic pile bending moment under different ground conditions are proposed in this study. Notably, this study presents the first attempt to validate and modify these simplified models specifically for triple-layered ground through comprehensive 3D numerical parametric analysis. Compared with existing models that are mainly applicable to uniform or double-layered ground, the empirical formulas proposed in this study demonstrate applicability for both double-layered and triple-layered ground conditions, significantly enhancing the prediction accuracy of kinematic bending moments of piles under seismic loading in complex ground systems.

Keywords: empirical model; feasibility evaluation; kinematic bending moments; numerical modeling; pile group; seismic analysis

1. Introduction

Piles are widely used in civil engineering to transfer loads to stable geological formations, and their behavior under seismic excitations must be evaluated in engineering practice (Sica *et al*. 2007). Under seismic excitations, pile foundation is subjected to two distinct forces: the first being the oscillations of the superstructure (*inertial force*), and the second being the dynamics of pile-soil interactions (*kinematic force*). In the conventional design approaches, pile foundations are typically engineered to resist the *inertial forces* that arise from the superstructure's oscillatory movement, while the *kinematic forces* generated by seismic-wave transmission through the soil deposit are often overlooked (Luo *et al*. 2021). The maximum kinematic bending moment at pile head has received considerable attention, as this is typically the primary cause of damage to a pile under seismic loading. However, it was also determined that the effects of the kinematic interaction have the potential to cause severe damage to a pile in the proximity of interfaces between soil strata where sharp stiffness variation occurs. It has been demonstrated through observations of previous devastating earthquakes and dynamic centrifuge experiments that kinematic forces play a significant role in the development of pile damage (Garala and Madabhushi 2021, Tott-Buswell *et al*. 2022). Seismic regulations, such as Eurocode 8 (2023), have acknowledged the significance of kinematic effects. These regulations stipulate the necessity of incorporating both inertial and kinematic interactions in pile design under specific circumstances, including the ground profile type, the site's seismicity, and the structural importance.

A number of research efforts, including analytical methods (Dobry and O'rourke 1983, Mylonakis 2001, Nikolaou *et al*. 2001, Di and Rovithis 2015, Ke and Zhang 2017, Misirlis *et al*. 2019, Alamo *et al*. 2020, Di 2023), experimental tests (Garala and Madabhushi 2021, Meymand 1998, Boulanger *et al*. 1999, Kagawa *et al*. 2004, Banerjee *et al*. 2014, Fatahi *et al*. 2014, Chidichimo *et al*. 2014, Zhang *et al*. 2017) and numerical simulations (Luo *et al*. 2021, Dezi *et al*. 2010, Sica *et al*. 2011, Di *et al*. 2013, Hussien *et al*. 2015, Dezi and Poulos 2017, Vignesh and Muttharam 2023, Martinelli *et al*. 2016) have been undertaken over the past decades to examine the kinematic effects of seismically excited piles. Analytical methods,

*Corresponding author, Professor
E-mail: btangzh@ecjtu.edu.cn
[a]Ph.D.
[b]Ph.D. Student
[c]Ph.D.

Copyright © 2025 Techno-Press, Ltd.

ISSN: 2005-307X (Print), 2092-6219 (Online)

including the Beam on Dynamic Winkler Foundation model (BDWF) (Mylonakis 2001, Di and Rovithis 2015), the dynamic *p-y* method (Boulanger *et al*. 1999, Kagawa *et al*. 2004), and the pseudo-static method (Liyanapathirana and Poulos 2005, Castelli and Maugeri 2009, Elahi *et al*. 2010) are widely adopted to evaluate the seismic pile-soil interaction. However, as discussed by Zhang *et al.* (2017), the precision of these analytical techniques depends on the input parameters, which are frequently derived from the back-calculation of measured pile response.

Numerical methods, including three-dimensional finite element (FE) and finite difference (FD) approaches (Misirlis *et al*. 2019, Alamo *et al*. 2020, Bouckovalas and Chaloulos 2014, Hokmabadi *et al*. 2014, Mánica *et al*. 2016), have also been widely employed to examine the seismic pile-soil interaction. Although a series of advanced soil constitutive models have been developed to consider the effects of strain degradation and softening of soil stiffness and strength, in addition to geometric and hysteretic damping, these models are computationally intensive and time-consuming, which has precluded the application of the numerical methods among professional engineers with limited time and budgets. Centrifuge and shaking table tests are also employed to analyze the seismic response for pile foundations. These experimental approaches can reveal the realistic seismic pile-soil interaction. However, sophisticated experimental skills are needed for reliable data. Additionally, centrifuge or shaking table tests are rather time and money-consuming, which is not realistic for practical engineering design, and are instead mainly used for case validation.

A series of theoretical, experimental, and numerical research (Garala and Madabhushi 2021, Mylonakis 2001, Misirlis *et al*. 2019, Dezi *et al*. 2010, Di *et al*. 2013) have demonstrated that the peak kinematic bending moment occurs at the vicinity of interfaces between soil strata with sharp stiffness variation. To facilitate the initial design of piles in seismic conditions, various simplified approaches or analytical methodologies have been advanced to estimate the maximum kinematic bending moment at the soil interfaces. The simplified models are quite handy since most of them have been validated by analytical or numerical calculations for a broad range of soil conditions, and can be considered a suitable option for engineering purposes (Misirlis *et al*. 2019, De and Maiorano 2010, Maiorano *et al*. 2009). However, most of these simplified approaches are primarily based on idealized uniform or two-layered ground conditions, and there remains a significant research gap concerning triple-layered or more complex multilayer ground profiles. In triple-layered ground, the mechanisms of shear wave propagation, reflection, and pile-soil interaction across different layers can lead to a more complicated distribution of pile bending moment, making it difficult for existing models to accurately capture the location and magnitude of the maximum bending moment. For instance, centrifuge tests (Huded and Dash 2024) on piles in complex grounds reveal that intermediate layer can significantly alter the depth of the maximum bending moment. Moreover, the stiffness and thickness of the intermediate layer may significantly change the stress transmission path, thereby affecting both the depth and magnitude of the maximum bending moment. For instance, centrifuge model tests have shown that the bending moment distribution patterns of piles in multilayered soils are governed by the position of the interlayer, which is markedly different from the response observed in homogeneous soils (Chen *et al.* 2024). Therefore, investigating the kinematic bending moment distribution patterns of piles in triple-layered ground conditions not only helps bridge the existing research gap but also contributes to improving the design accuracy of pile foundations in complex ground conditions under seismic loading.

In this paper, several commonly used simplified approaches for the estimation of maximum kinematic pile bending moment are reviewed, and a parametric numerical analysis is carried out, aiming to propose a wider applicable model for predicting the maximum kinematic pile bending moment in complex ground conditions. Firstly, the distribution characteristics of kinematic bending moment for the single pile and pile group are analyzed, and the influences of the seismic motion, pile dimensions, and ground conditions on the maximum kinematic bending moment are investigated. Utilizing the comprehensive parametric numerical investigations, the feasibility and reliability of the simplified approaches are evaluated, and several simplified formulae are proposed for estimating the maximum kinematic pile bending moment in both double-layered and triple-layered ground conditions

2. Review of simplified models and methodology of this study

2.1 Review of simplified models

To provide an explicit design formula for seismic pile design, simplified models have been proposed for predicting the maximum kinematic bending moments of piles under seismic loading. As demonstrated in Table 1. several commonly utilized simplified models are reproduced, for more details refer to Dobry and O'Rourke (1983), Mylonakis (2001), Nikolaou *et al.* (2001), and Maiorano *et al.* (2009). The presented simplified models are proposed based on BDWF or numerical models and are applicable to the double-layered ground, in which a soft stratum was underlined by a stiff stratum. These simplified models mainly consider the pile dimensions, soil, pile stiffnesses, period of the input motion period, and thus the maximum kinematic bending moments of piles at the soil interfaces can be easily obtained by inputting the readily dimensional and stiffness parameters.

However, as the simplified models are empirically derived, their accuracy in practical engineering applications is highly contingent upon the correspondence between actual site conditions and the original calibration scenarios. These models universally assume a double-layered ground condition with moderate shear wave velocity contrasts between strata. When actual geological conditions deviate significantly from these idealized assumptions, the

Table 1 Summary of simplified models

No.	model descriptions	model parameter	parameter description	model origin	ground type	Reference
S1	$M=1.86(E_PI_P)^{3/4}\cdot G_1^{1/4}\cdot\gamma_1\cdot F$	$F=\frac{(1-c^{-4})(1+c^3)}{(1+c)(c^{-1}+1+c+c^2)}$ $\gamma_1=\frac{r_d\cdot\rho_1\cdot H_1\cdot a_{\max S}}{G_1}$ r_d=1-0.015z $c=(\frac{G_2}{G_1})^{1/4}$	$a_{max,S}$: maximum acceleration at the soil surface d: pile diameter E_p: pile elastic modulus E_1: elastic modulus of upper layer F: dimensionless function of the ratio of the shear moduli of the two layers G_1: shear modulus of upper layer G_2: shear modulus of lower layer H_1: thickness of upper layer H_2: thickness of lower layer I_p: pile inertia moment k_1: soil–spring stiffness L: pile length r: pile radius V_{S1}: shear wave velocity of upper layer V_{S2}: shear wave velocity of lower layer φ: amplification factor accounting for excitation frequency, typically less than 1.25, 1.0 for preliminary design φ^*: amplification factor, 1.39 and 1.30 for resonant and non-resonant conditions, respectively β: coefficient, 0.075 and 0.069 for resonant and non-resonant conditions, respectively ε_p: bending strain at the outer fiber of the pile cross section v: Poisson's ratio of soil γ_1: maximum soil shear strain at the interface γ_1^*: maximum soil shear strain at the interface, calculated by EERA r_d: depth factor ρ_1: density of the upper layer τ_c: characteristic shear stress at the interface τ_c^*: characteristic shear stress at the interface, calculated by EERA z: depth of interface	single pile BDWF model	Double-layered	Dobry and O'Rourke (1983)
S2	$M=\frac{(E_PI_P)\cdot(\varepsilon_P/\gamma_1)}{r}\phi\cdot\gamma_1$	$\frac{\varepsilon_P}{\gamma_1}=\frac{1}{2c^4}(c^2-c+1)(\frac{H_1}{d})^{-1}$ $\left\{[3(\frac{k_1}{E_P})^{1/4}(\frac{H_1}{d})-1]\cdot c(c-1)-1\right\}$ $\delta=\frac{3}{1-v^2}(\frac{E_P}{E_1})^{-1/8}(\frac{L}{d})^{1/8}(\frac{H_1}{H_2})^{1/12}(\frac{G_1}{G_2})^{-1/30}$ $c=(\frac{G_2}{G_1})^{1/4}$ $\gamma_1=\frac{r_d\cdot\rho_1\cdot H_1\cdot a_{\max S}}{G_1}$ $k_1=\delta E_1$		single pile BDWF model	Double-layered	Mylonakis (2001)
S3	$M=0.042\cdot\tau_C\cdot d^3(\frac{L}{d})^{0.30}(\frac{E_P}{E_1})^{0.65}(\frac{V_{S2}}{V_{S1}})^{0.50}$	$\tau_C=\rho_1\cdot H_1\cdot a_{\max S}$ $\frac{\varepsilon_P}{\gamma_1}=\frac{1}{2c^4}(c^2-c+1)(\frac{H_1}{d})^{-1}$ $\left\{[3(\frac{k_1}{E_P})^{1/4}(\frac{H_1}{d})-1]\cdot c(c-1)-1\right\}$		single pile BDWF model	Double-layered	Nikolaou *et al.* (2015)
S4	$\frac{M}{a}=\phi^*\cdot\gamma_1^*$ $\frac{M}{b}=\beta\cdot\tau_C^*$	$b=\frac{0.5}{1+v}\cdot d^3(\frac{L}{d})^{0.30}(\frac{E_P}{E_1})^{-0.35}(\frac{V_{S2}}{V_{S1}})^{0.50}$ $a=\frac{E_PI_P}{r}(\frac{\varepsilon_P}{\gamma_1})$		single pile 3D numerical models	Double-layered	Maiorano *et al.* (2009)

applicability of such simplified approaches remains to be fully ascertained. For instance, the triple-layered ground with a soft intermediate layer – frequently encountered in practice due to complex depositional histories – represents a notable knowledge gap. Current research provides insufficient analysis of kinematic bending moment distributions under such configurations, and the validity of existing simplified methods for these conditions warrants rigorous verification.

For the simplified models to be more widely accepted in practical pile foundation designs, the feasibility and reliability of the simplified models must be evaluated thoroughly, whilst also conducting a comprehensive examination of their applicability to more complex ground conditions.

2.2 Methodology of this study

The methodological framework adopted in this research employs a comprehensive numerical approach to evaluate the maximum kinematic bending moments for pile foundations subjected to seismic loading within layered ground conditions, with particular emphasis on triple-layered strata. The study integrates three-dimensional (3D) explicit finite difference modeling, systematic parametric analysis, and rigorous validation protocols to achieve its objectives. The methodology is structured into four interconnected phases: (1) numerical model development and calibration, (2) parametric investigation, (3) evaluation of existing simplified models, and (4) formulation and validation of enhanced predictive equations.

Firstly, the numerical model was calibrated using the benchmark case of Sanctis *et al*. (2010). Validation was performed through comparative analysis of the distributions of kinematic bending moments along the pile shaft and soil accelerations with depth. On this basis, a systematic parametric study was conducted to evaluate the accuracy of existing simplified models in predicting maximum kinematic bending moments for piles in both double-layered and triple-layered ground conditions. The parametric variations encompass pile diameter, ratios of shear wave velocities between soil layers, and stratum thicknesses. Notably, this study presents the first attempt to investigate the maximum kinematic bending moments in the triple-layered ground with a soft intermediate layer. The influence of key parameters – particularly the thickness and shear wave velocity of the intermediate soft layer – was rigorously examined. Parametric results demonstrate that while the Maiorano *et al*. (2009) method provides reasonably accurate predictions for double-layered ground, it yields significant errors (>20%) for triple-layered ground.

Finally, a simplified empirical formula applicable to triple-layered ground was developed by extending the Maiorano *et al.* (2009) framework. The proposed method's reliability was verified against numerical results, with all deviations in predicted maximum kinematic bending moments remaining within 20%.

3. Numerical model for seismic analysis

3.1 Numerical model validation

To validate the numerical modeling, a case studied by

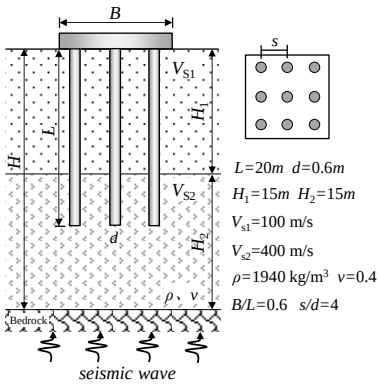

Fig. 1 Case for the validation of the numerical model

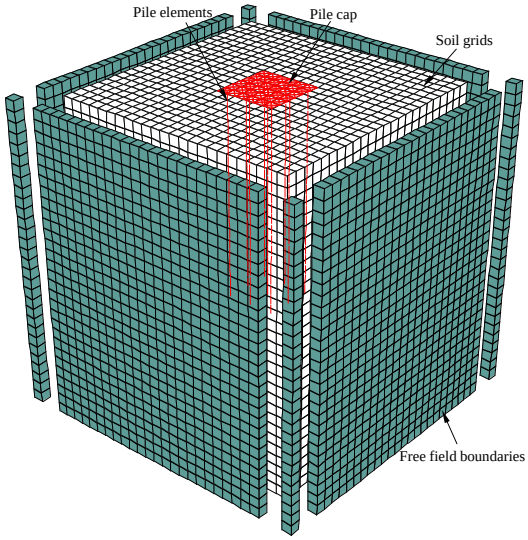

Fig. 2 Mesh of the validation model

Sanctis *et al.* (2010) is used, as shown in Fig. 1. The ground consists of two 15 m thick soil strata underlain by a rigid base at H = 30 m. The soil shear wave speeds are V_{S1} = 100 m/s for the upper soft stratum and V_{S2} = 400 m/s for the lower hard stratum. A soil density ρ of 1940 kg/m^3 and Poisson's ratio v of 0.4 are postulated in the case of the two strata. A 3×3 pile group is investigated with pile length L = 20m, spacing s = 4d, and diameter d = 0.6 m. The pile material Young's modulus E_P = 25 GPa and the pile head is presumed to be fixed against rotation. The pile cap is square with a width B = 12 m and is assumed as a rigid body in this case. Consistent with previous studies (Zhang *et al*. 2022, Zheng *et al*. 2022, Zhang *et al*. 2025), this research employs a linear elastic constitutive model to simulate soil behavior, aiming to balance computational efficiency and accuracy. Specifically, under minor seismic conditions where soil nonlinear effects are negligible, the linear elastic model can effectively reduce computational complexity while ensuring analytical accuracy.

Fig. 2 displays the structured finite-difference meshes of the validation model with 20280 hexahedral zones and 26071 grids in total. The boundary conditions are selected to reflect the semi-infinite nature of the ground conditions, i.e., the side grids are free field boundaries. The free-field boundaries involve performing free-field calculations alongside the analysis of the main-grid (soil grids). The secondary grid (i.e., the free field boundary grid) is then coupled to the main-grid by viscous dashpots and the unbalanced forces are loaded onto the main-grid, thus forcing the free field motion at the boundary (Itasca 1997). In this model, the free field boundaries are placed two times the length of the pile cap away from the edge of the surface structure, following the suggestion given by Mánica *et al.* (2016). In the seismic analysis, a stiff boundary is employed to simulate the bedrock, as suggested by other researchers (Hokmabadi *et al*. 2014, Dutta and Roy 2002, Spyrakos *et al*. 2009), and the acceleration time series (A-TMZ000) is applied to the bedrock under the assumption of horizontal shear waves with vertical propagation. The following section details the input acceleration time histories and response spectra.

Consistent with the analysis performed by Sanctis *et al.* (2010), the soil was modeled by means of a linear elastic constitutive model. Use the following equations to determine the shear modulus G and bulk modulus K

$$G=\rho \cdot V_s^2 \tag{1}$$

$$K=\frac{2G(1+v)}{3(1-2v)} \tag{2}$$

Where ρ is soil density; V_s is shearing wave velocity; v is Poisson's ratio. The values of these parameters have been mentioned above.

Damping is a significant element in the seismic analysis of soil-structure interactions. The built-in Rayleigh damping is employed here. In FLAC^{3D}, Rayleigh damping is specified by two input parameters, i.e., the critical damping ratio ξ_{min} and central frequency f_{min}. Consistent with that in Sanctis *et al.* (2010), a critical damping ratio ξ_{min} of 10% is adopted. The central frequency f_{min} is set equal to the middle frequency (2.47 Hz in this study) between the lowest and highest predominant frequencies, as suggested by Itasca (1997) and Mánica *et al.* (2016).

For numerical computation time saving, structural elements rather than solid elements are adopted. The bending and axial stiffnesses of the pile elements are determined by the cross-sectional geometry and the stiffness parameters (Young modulus E_p and Poisson's ratio v_p). Similarly, the pile cap is emulated by the shell-type elements, and the bending stiffness is governed by the thickness and stiffness parameters (Young modulus E_R and Poisson's ratio v_R). The validation case considers the pile cap as a rigid cap devoid of self-weight, thus a density of 100 kg/m^3, a thickness of 0.1 m, Young modulus E_R of 200GPa is assumed. Notably, the density of 100 kg/m^3 is purely for the purpose of calculating stability, and the effect of the inertial force on the pile bending moment is minimal. The top nodes of the piles are tied to the pile cap by rigid links, thereby ensuring that the six degrees of freedom per node (three translational and three rotational components) are equivalent for both the pile nodes and the corresponding shell nodes. The analysis facilitates straightforward extraction of the internal force (e.g. bending moments) of the structural elements, and the structural elements' validity

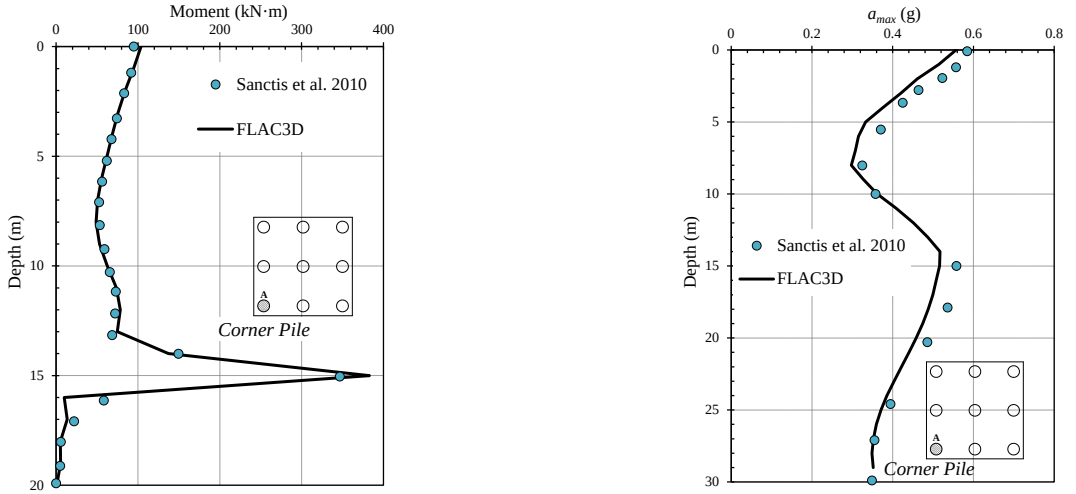

(a) pile bending moment envelope profile (b) soil acceleration envelope profile

Fig. 3 Comparison of the validation modeling and those by Sanctis *et al*. (2010)

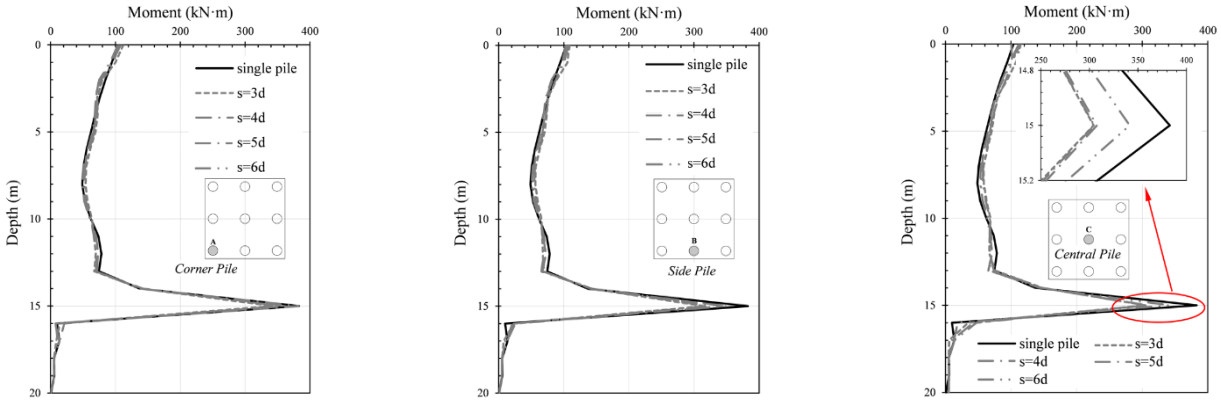

(a) Corner Pile (b) Side pile (c) Central pile

Fig. 4 Influence of pile spacing on the envelope profile of kinematic bending moment

and dependability were adequately substantiated in seismic soil-structure analyses by Mánica *et al.* (2016).

Linear spring systems constitute the modeling framework for the interactions between pile elements and the surrounding soil grids. In the FLAC^{3D} modeling framework, it is advised that the normal and shear stiffness parameters for the springs should be set to ten times the equivalent stiffness of the stiffest neighboring zone. The normal and shear stiffness k values are estimated by the following equation:

$$k = 10 \times \max\left(\frac{K + \frac{4}{3}G}{\Delta z_{\min}}\right) \tag{3}$$

Where K and G are the bulk and shear modulus, respectively; and z_{min} is the smallest width of an adjoining zone in the normal direction, 1m in this study.

Following the equation above, the values for the normal and shear stiffness of the springs are rounded up to 1×10^8 kPa.

Fig. 3 illustrates the pile moment and soil acceleration envelope profiles evaluated by Sanctis *et al.* (2010) and FLAC3D modeling here, which shows a rather well agreement and validates the numerical model adopted by this study. As illustrated in Fig. 3(a), the kinematic pile bending moments are pronounced, particularly near the soil layer interface. A spike bending moment of approximately 400 kN·m is observed, underscoring the significance of incorporating kinematic force in the design of pile foundations in seismic areas.

3.2 Kinematic pile bending moment of single pile and pile group

Following the validation of the numerical model above, a series of pile groups with varying spacing and a range of piles are further examined, and the distribution of kinematic pile bending moment is investigated within the pile group. Same with that in the validation case, the acceleration time series (A-TMZ000) is applied to the bedrock. The ground conditions and pile dimensions are consistent with those in the validation model, and the model parameters and the numerical modeling issues can be referred to the section above.

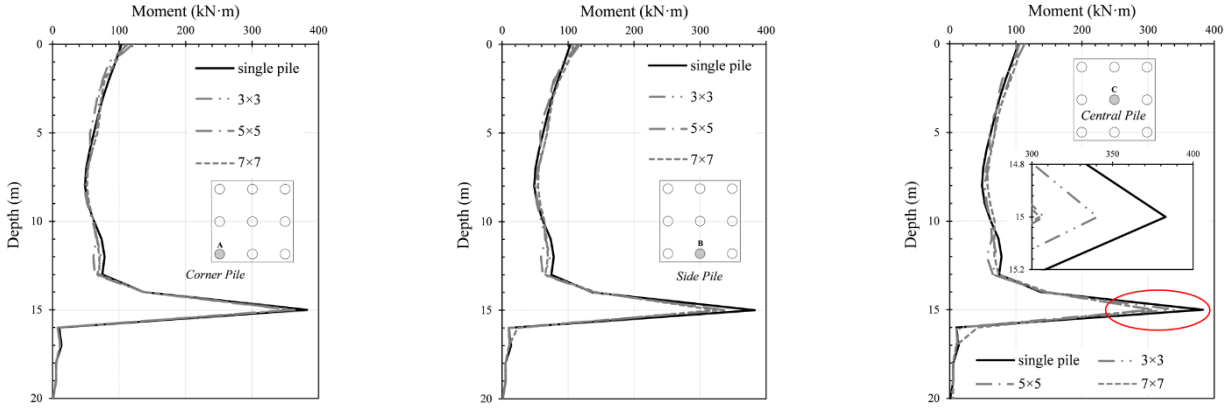

(a) Corner Pile (b) Side pile (c) Central pile

Fig. 5 Impact of number of piles on the envelope profile of kinematic bending moment

Fig. 4 presents the influence of pile spacing on the envelope profile of the kinematic bending moment. Pile spacing exerts a minor influence on the envelope profile of kinematic bending for the pile group, and the kinematic bending moment distribution is very similar to that of the single piles along the entire length. Similar with the numerical results obtained by Dezi and Poulos (2017), the group effect is obvious at the interface with soil stiffness changing sharply, and the reductions in kinematic bending moments are pronounced near the interfaces of soil strata.

The impact of pile number in a group on the envelope profile of the maximum kinematic bending moment is presented in Fig. 5. The distribution of the maximum kinematic bending moment is found to be highly comparable among in the corner, side piles and the single pile. The reduction in kinematic bending moments mainly occurred near the interfaces of soil strata for the central pile. The discrepancy observed in the maximum kinematic bending moment between a single pile and the central pile is within 26%.

From the numerical results presented in Figs. 4 and 5, it can be seen that due to the shading effect of adjacent piles, the maximum kinematic bending moment borne by the pile shaft at the soil layer interface in the pile group foundation is lower than that of a single pile in the free field, with a maximum reduction of approximately 26%. Based on this characteristic, using the pile shaft bending moment results of a single pile foundation in practical engineering design can meet safety requirements, and the design is conservative.

In addition, the number of piles and pile spacing have certain influences on the pile group effect. Overall, a larger number of piles and smaller pile spacing lead to a more pronounced pile group effect and a smaller maximum kinematic bending moment in the pile shaft; however, corresponding critical values exist. For instance, considering the center pile, once the pile group configuration reaches 5×5, further increasing the number of piles does not cause a significant attenuation in its maximum kinematic bending moment. Similarly, when the pile spacing is below $5d$ (where d is the pile diameter), further reduction in spacing has a negligible effect on the maximum kinematic bending moment at the soil layer interface.

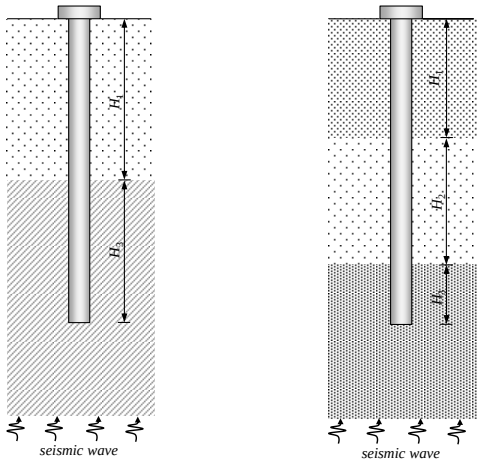

(a) Double-layered ground (b) Triple-layered ground

Fig. 6 Ground conditions

3.3 Parametric study

As discussed above, the seismic pile design based on a single pile can be regarded as a conservative design. For computation time saving, the parametric study is all based on a single pile. To more realistically represent the restraining effect of the raft on the pile head, the pile head in the parametric analyses is assumed to be restrained from rotation but permitted to undergo corresponding horizontal displacement and can be considered as a form of partial fixity.

3.3.1 Ground conditions

As presented in Fig. 6, two types of ground conditions are examined. For double-layered ground, with a soft stratum underlined by a stiff stratum, is employed in this study. Besides, a triple-layered ground, in which a soft stratum is sandwiched between two stiff strata, is adopted to examine the applicability of these simplified models when applied to more complex ground conditions.

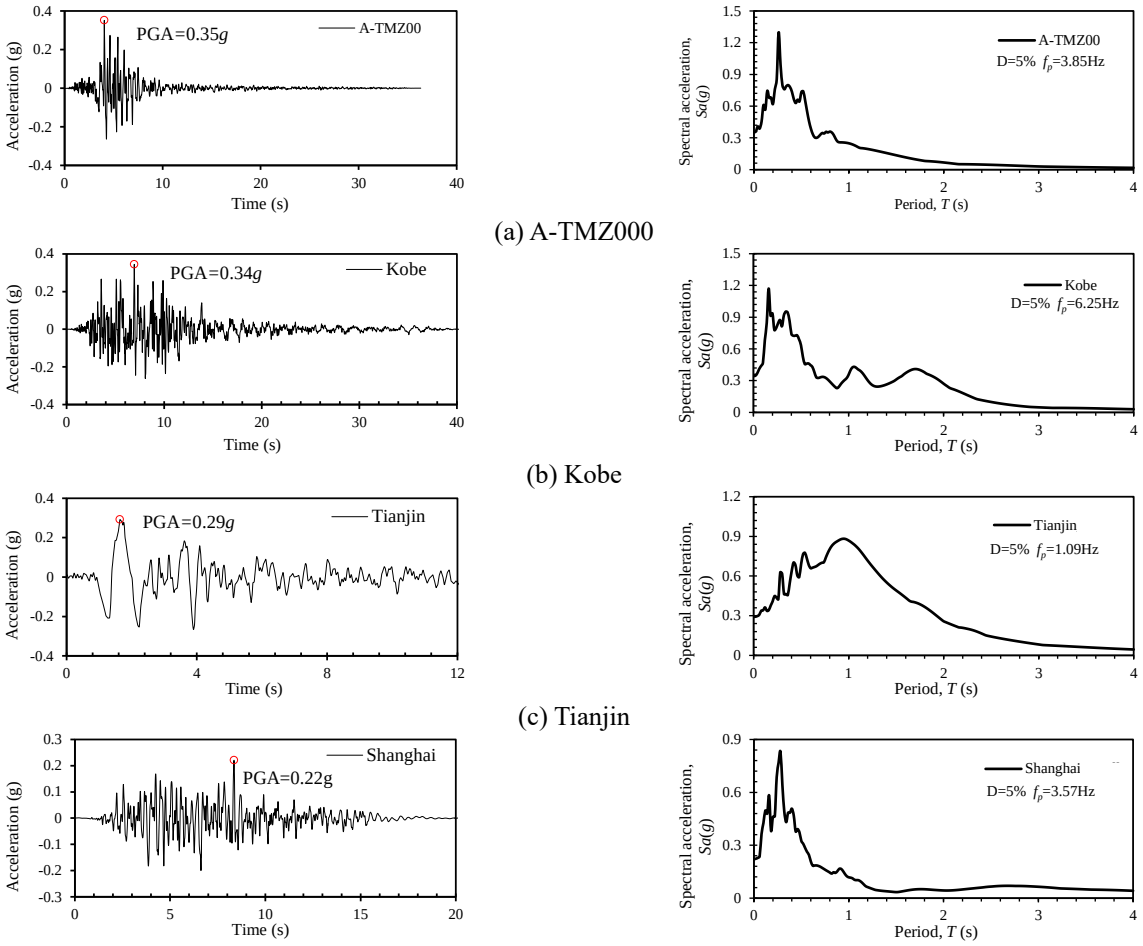

Fig. 7 Acceleration time histories and response spectra at the bedrock roof

3.3.2 Seismic motions

Fig. 7 shows the acceleration time histories of the four seismic motions as well as the corresponding associated response. The peak ground accelerations (PGA) of the four seismic motions range from 0.22~0.35g, and the seismic peak frequency f_p ranges from 1.09~6.25 Hz. As the parametric study is focusing on the evaluations of the simplified models, rather than investigations of the specific case under designated acceleration time histories, the seismic acceleration time histories at the bedrock are applied without deconvolution analysis from the outcropping rock to the roof of the bedrock.

3.3.3 Analysis cases

The cases pertaining to the double-layered and triple-layered ground are presented in Appendix Table 1 and Appendix Table 2. In both cases, the pile and soil properties are as follows: L=20 m, E_P =25 GPa, v_p=0.2, ρ_s =1940 kg/m^3, v = 0.4.

For the double-layered ground, a total of 28 cases is examined on the pile kinematic bending moment with varying shear wave velocities (V_{S1} = 60~200 m/s and V_{S2} = 200~400 m/s) thickness of top soil stratum H_1 (from 5 m to 15 m), pile diameter d (0.3 m to 1.0 m) and soil damping ratio D (2% to 10%). For the triple-layered ground, a total of 28 cases is also investigated with the upper strata shear wave velocity V_{S1} =100~300 m/s, the middle soft layer V_{S2} = 50 or 100 m/s, and 400 m/s for the bottom stiff layer. The thickness of the middle soft layer H_2 is 10 m, and the thickness of the first layer H_1 ranges from 2 to 10 m to make sure the layer interface is not beyond the pile length. The pile diameter d is 0.6 m or alternatively 1 m, and the soil damping ratio D is 10%.

The summary of the analysis cases can be found in Appendix Table 1 and Appendix Table 2, respectively for the double-layered and triple-layered grounds. The four acceleration time histories mentioned above are applied at the bedrock for each case, resulting in a total of 224 cases analyzed.

4. Results and discussions

4.1 Distribution of kinematic bending moment

As shown in Figs. 6 and 9 are the envelope profiles of the maximum pile bending moments induced by the kinematic interactions in the two grounds. As previously observed in the validation model, spike kinematic bending moments are present in the vicinity of the interfaces

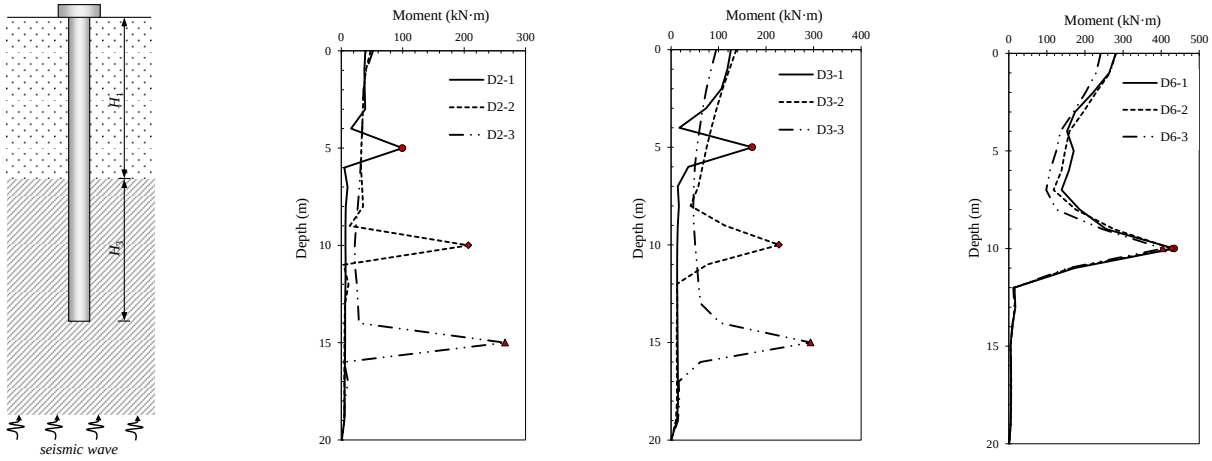

Fig. 8 Envelope profile of kinematic pile bending moment for double-layered ground (Kobe)

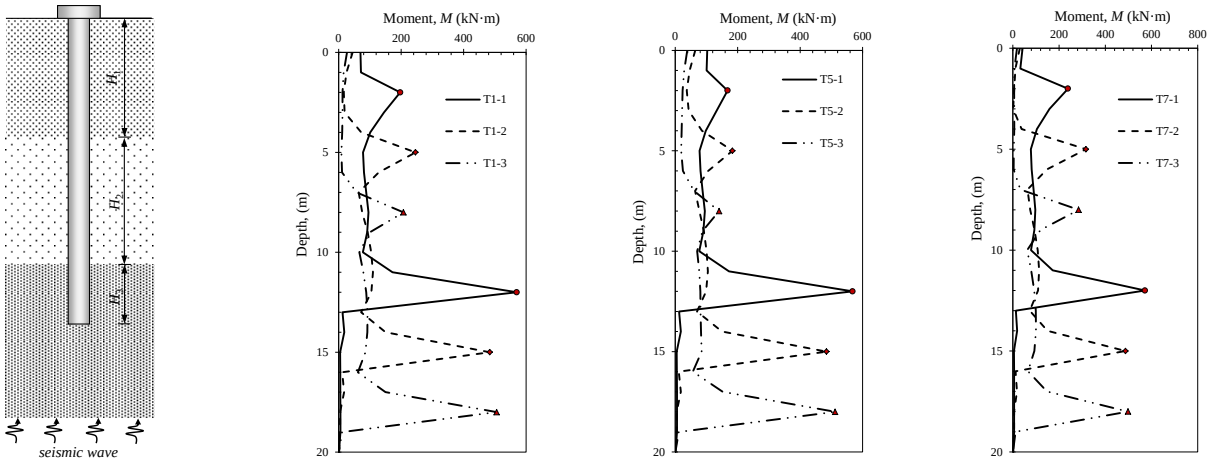

Fig. 9 Envelope profile of kinematic pile bending moment for triple-layered ground (Kobe)

between the soil strata. For the double-layered ground, the spike kinematic bending moments at the interface increase with the increasing thickness of the upper soil stratum. When the upper soil is thin, the kinematic bending moment at the pile head becomes more prominent than that at the soil interface.

As presented in Fig. 9, the envelope profile has two spike kinematic bending moments at the interfaces in triple-layered ground. The kinematic bending moment at the lower soil interface exhibits a significantly higher value than that at the upper soil interface. Unlike the distribution in the double-layered ground, the kinematic bending moment at the soil interfaces is found to be independent of the thickness of the upper soil stratum, and the kinematic bending moment at the pile head is observed to be considerably smaller than those at the soil interfaces.

4.2 Evaluations of the simplified models

4.2.1 Double-layered ground

The comparisons between the numerical kinematic bending moment at the soil interface *Mc* and that predicted by the simplified model by Dobry and O'Rourke (1983) M_p is demonstrated in Fig. 10. The data indicates that the ratio

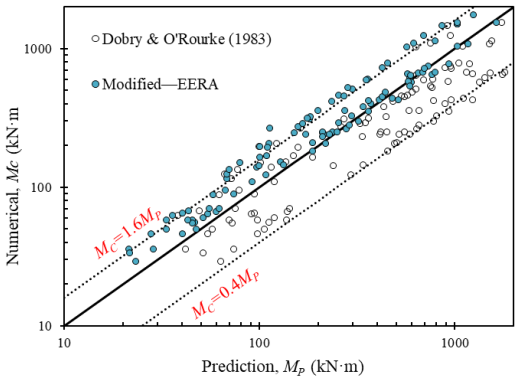

Fig. 10 Comparison of numerical and prediction by Dobry and O'Rourke in double-layered ground

of M_c/M_p is mainly ranging from 0.4~1.6, with an error of approximately 60%. As illustrated in Table 1, the maximum soil shear strain at the interface γ_1 originally calculated by the method proposed by Seed and Idriss (1982). Bardet *et al.* (2000) argued the recommendation by the EERA code for the maximum soil shear strain is more accurate. The comparison has been conducted between the numerical results and that predicted by Dobry and O'Rourke (1983)

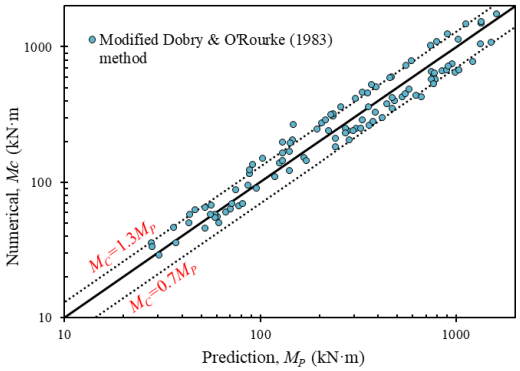

Fig. 11 Comparison of numerical results with modified Dobry and O'Rourke model

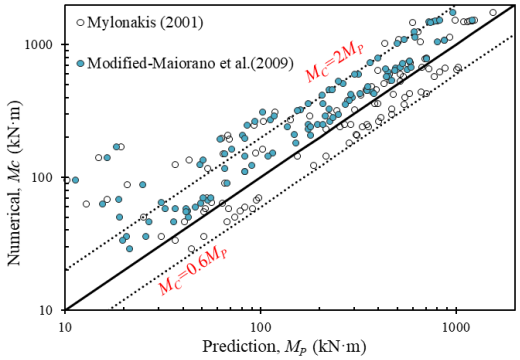

Fig. 12 Comparison of numerical results with prediction by Mylonakis and Maiorano models

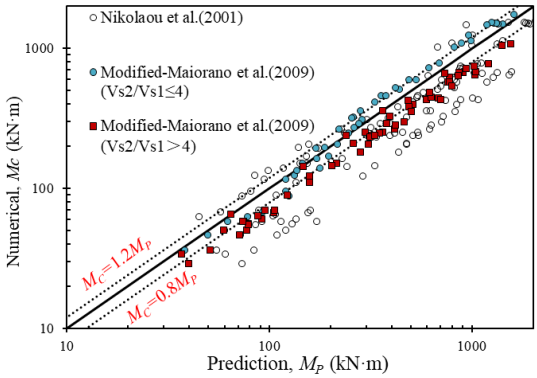

Fig. 13 Comparison of numerical and prediction results (Nikolaou *et al.* 2001 and Maiorano *et al*. 2009)

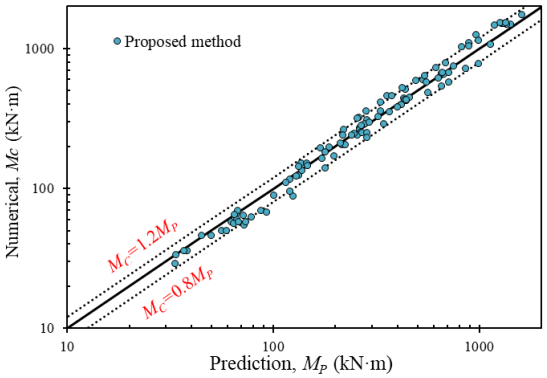

Fig. 14 Comparison of numerical results with prediction by modified model in double-layered ground

model with γ_1 evaluated by the EERA code is also presented in Fig. 10. It is evident that the modified model demonstrates enhanced prediction accuracy, with the ratio of M_c/M_p mainly ranging from 1.0~1.6.

As discussed above, the Dobry and O'Rourke (1983) model with γ_1 evaluated by the EERA code will underestimate its kinematic bending moment at the soil interface. To improve the prediction accuracy, a further modified Dobry and O'Rourke model (1983) have proposed, as Eq. (4.1)

$$M = 2.42 \cdot (E_P I_P)^{3/4} \cdot G_1^{1/4} \cdot \gamma_1 \cdot F \tag{4}$$

Where γ_1 is the maximum soil shear strain at the soil interface and is obtained by EERA code; descriptions of the other parameters can be referred to Table 1.

The comparison between the numerical findings and those predicted by Eq. (4.1) is presented in Fig. 11, which shows a well agreement with the ratio of M_c/M_p mainly ranging from 0.7~1.3.

The comparison of the numerical results with those predicted by Mylonakis (2001) and Maiorano *et al.* (2009) are presented in Fig. 12. It can be seen that, except for some scattered data for smaller M_p, the ratio of M_c/M_p for both two models mainly range from 0.6 ~ 2.0 and 1.0 ~ 2.0, respectively.

A comparison of the numerical results with those predicted by Nikolaou *et al.* (2001), and the modified model by Maiorano *et al.* (2009) is presented in Fig. 13. As can be observed, the modified models by Maiorano *et al.* (2009) have a much higher prediction accuracy compared to the Nikolaou *et al.* (2001) model, with the ratio of M_c/M_p mainly ranging from 0.8~1.2 for cases with shear wave velocity ratio $V_{S2}/V_{S1} \le 4$, and a little bit larger variation for cases with shear wave velocity ratio $V_{S2}/V_{S1}>4$.

As discussed above, the modified Maiorano model will overestimate the pile kinematic bending moment for cases with shear wave velocity ratio $V_{S2}/V_{S1} > 4$. To broaden the application scope of the modified Maiorano model, the simplified model is further modified as below

$$M = 0.069 \cdot f \cdot d^3 \left(\frac{L}{d}\right)^{0.3} \left(\frac{E_p}{E_1}\right)^{0.65} \left(\frac{V_{s2}}{V_{s1}}\right)^{0.5} \tau_C \tag{5}$$

Where: τ_c is the characteristic shear stress at the soil interface, and is calculated by EERA code; f is the correction factor for shear wave velocity ratio V_{S2}/V_{S1} and is estimated as follows

$$f = \begin{cases} 1 & V_{S2}/V_{S1} \le 4 \\ \left(\dfrac{4}{V_{S2}/V_{S1}}\right)^{0.9} & V_{S2}/V_{S1} > 4 \end{cases} \tag{6}$$

The present numerical outputs are then compared with the predictions of the proposed model, i.e., Eqs. (4.2) and (4.3), which is presented in Fig. 14. The ratio of M_c/M_p mainly ranges from 0.8~1.2, indicating the modified model can yield a rather well prediction for the maximum kinematic bending moments.

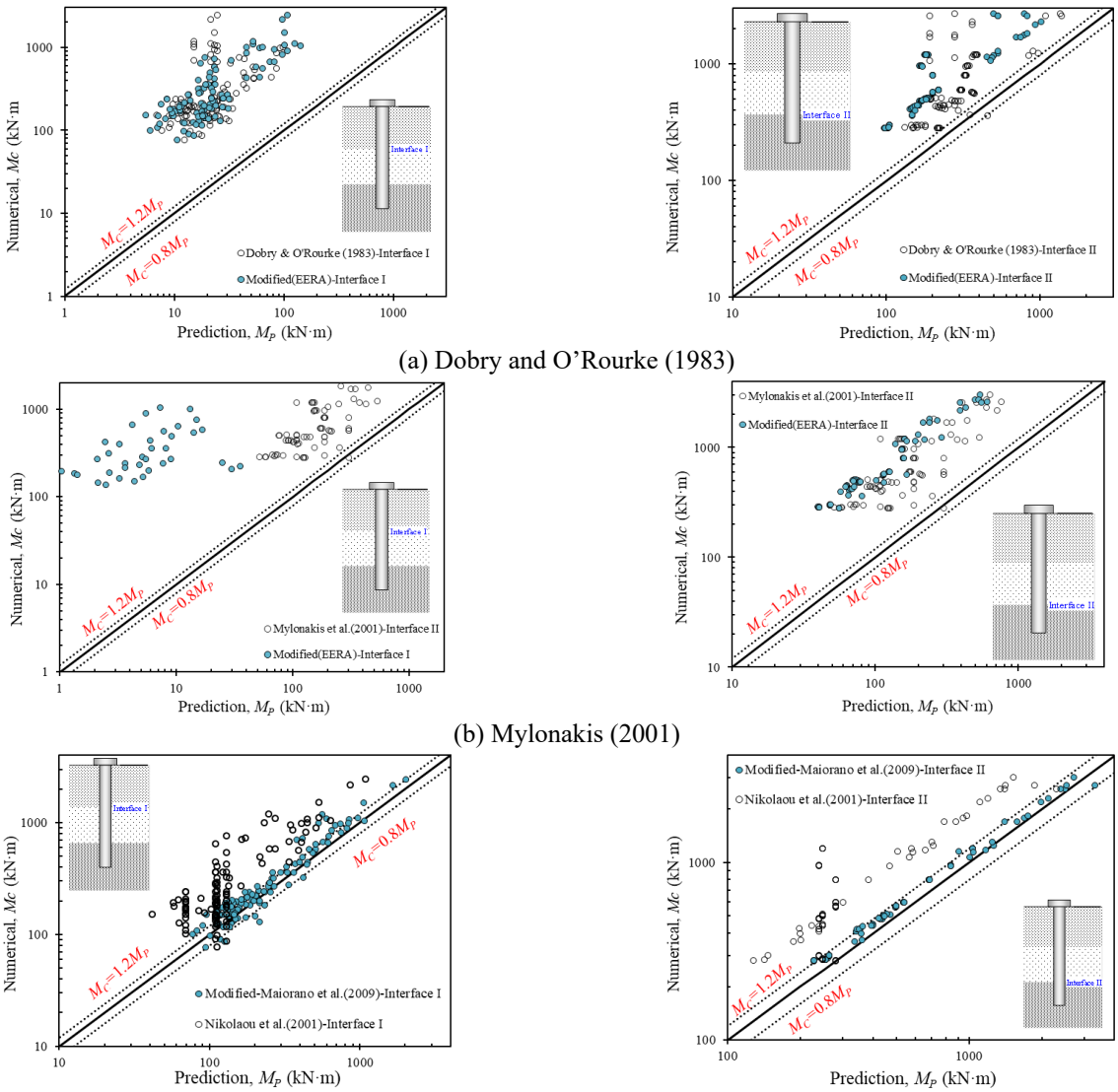

(a) Dobry and O'Rourke (1983)

(b) Mylonakis (2001)

(c) Nikolaou *et al*. (2001)

Fig. 15 Comparison of numerical results with predictions in triple-layered ground

4.2.2 Triple-layered ground

The comparisons of the present numerical results with those predicted by the simplified models for both interfaces (upper interface and lower interface) are presented in Fig. 15. As demonstrated in Fig. 15, the modified Nikolaou model proposed by Maiorano *et al.* (2009) exhibits enhanced accuracy, with the ratio of M_c/M_p mainly ranging from 0.8~1.2. Except for the modified Maiorano model, other simplified models all failed to predict the kinematic moments for the soil interfaces in the triple-layered ground. It should be pointed out that due to the presence of the sandwiched soft stratum, the ratio of the shear modulus between two layers and the strain transmissibility ε_p/γ_1 originated from double-layered ground as presented in Dobry and O'Rourke (1983) and Mylonakis (2001) may be invalid in the triple-layered ground, thus resulting in poor prediction for the kinematic bending moment in the triple-layered ground. The characteristic shear stress at the interface τ_c is connected to the kinematic bending moment in the modified Nikolaou model proposed by Maiorano *et al.* (2009), and it can be well estimated by the EERA code for both double or triple-layered ground, thus yielding more accurate prediction.

Based on the evaluations above, it can be concluded that the modified Nikolaou model proposed by Maiorano *et al.* (2009) is more accurate for the kinematic moment in both the double or triple-layered ground, with the ratio of M_c/M_p mainly ranging from 0.8~1.2, and it is recommended for seismic pile foundation design in practical engineering.

4.3 General design procedures

The usage process of the empirical formula models for predicting the maximum kinematic bending moments in double-layered and triple-layered ground is shown in the following figure.

4.4 Limitations and applicability of the model

While the proposed simplified model for estimating the

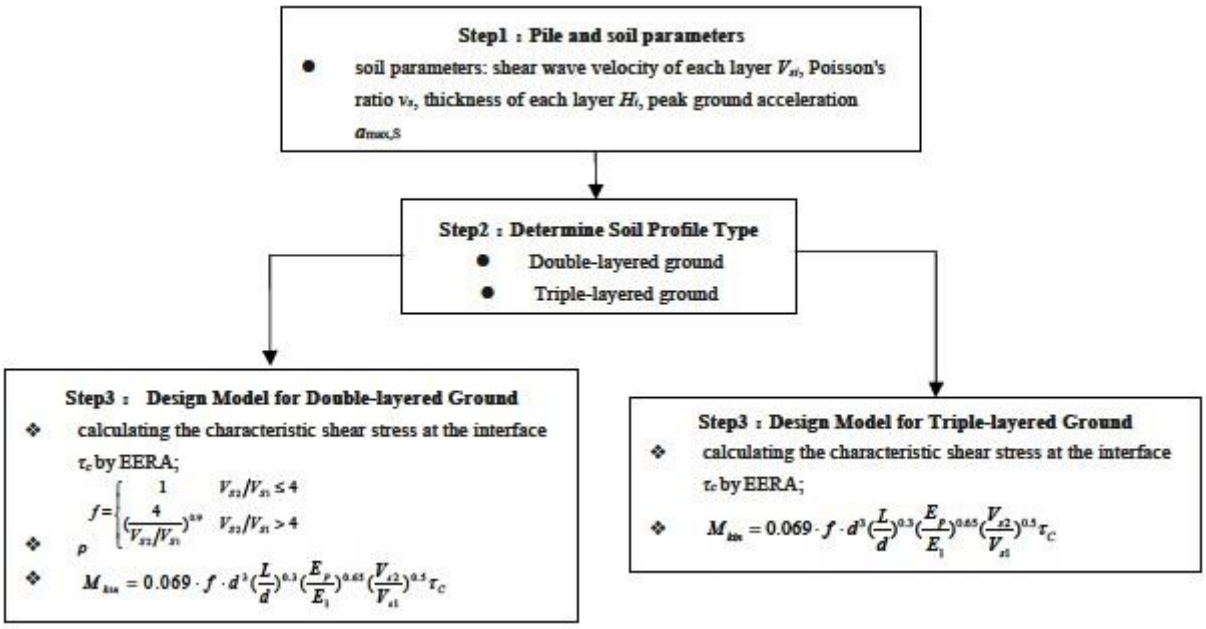

Fig. 16 Flowchart for the application of the empirical formulas

maximum kinematic pile bending moment under complex ground conditions (especially triple-layered ground) has demonstrated high prediction accuracy in comparison with numerical simulation results, the following limitations should be acknowledged:

1. Linear elastic model for ground soil: In this study, the linear elastic model was chosen for its higher computational efficiency, which effectively meets the computational cost of large-scale parametric analysis. In scenarios involving minor earthquakes, where nonlinear effects are negligible, it can balance the computational cost to deliver reliable results. However, this model may exhibit remarkable error in simulating strong earthquakes. It cannot capture nonlinear mechanical behaviors such as hysteresis in stress-strain curves, modulus degradation, or plastic strain accumulation, potentially leading to systematic biases in seismic response analyses. Nonlinear effects in strong earthquakes necessitate future extensions.

2. Lack of experimental validation: The simplified calculation methods for the maximum kinematic bending moment proposed in this paper are primarily derived from parametric numerical simulation analysis. However, it currently lacks systematic physical experimental validation, and further reliability verification analysis of the proposed method necessitates additional validation through centrifuge tests or shaking table tests.

3. Applicability boundaries: The simplified calculation method for the maximum kinematic bending moment of pile foundations proposed in this paper is mainly applicable to soft-stiff double-layered ground and triple-layered ground with a soft intermediate layer, and only for piles with fixed pile heads. If the above conditions are deviated from, the applicability or accuracy of the model needs to be considered carefully. For piles with free pile heads, or those located in liquefiable soil layers or unsaturated soil layers, the applicability of the model has not been verified. In addition, the prediction accuracy of the model may also be affected when the pile foundation is excessively long or has an irregular shape.

5. Conclusions

A series of three-dimensional numerical analyses are undertaken in this study to examine the kinematic soil-pile interactions. Notably, this is the first attempt to validate and modify simplified models in triple-layered ground using comprehensive 3D numerical parametric analysis. The feasibility of commonly used simplified models for estimating the maximum kinematic bending moment at the soil interfaces is evaluated. Based on the comprehensive parametric analysis, formulas are proposed for the estimation of the maximum kinematic pile bending moment in double-layered and triple-layered ground conditions. The main conclusions are drawn below:

- In the double-layered ground, the maximum kinematic bending moment increases with the increasing thickness of the upper soil stratum, while it is independent of the thickness of the upper soil layer in the triple-layered ground with a soft intermediate layer.
- The model proposed by Maiorano exhibits enhanced accuracy in estimating the maximum kinematic bending moment than other models when applied to the double-layered ground, with an error within 20% for cases with shear wave velocity ratio $V_{S2}/V_{S1} \le 4$. However, greater variation will occur for cases with $V_{S2}/V_{S1} > 4$.
- The empirical formula for predicting the maximum kinematic bending moment in triple-layered ground has been proposed. The predicted results fit well with numerical computations, with all deviations remaining below 20%, demonstrating good prediction accuracy and practical applicability for complex ground conditions.

Acknowledgments

The authors acknowledge the funding received from the National Natural Science Foundation of China (52568051, 52208343) and Natural Science Foundation of Jiangxi Province (20252BAC240359, 20232BAB214078) for supporting this research.

References

Alamo, G.M., Aznárez, J.J., Padrón, L.A., Maeso, O. and Gaitanaros, P. (2020), "Computation of pile kinematic bending moments in non-homogeneous soil profiles. Testing the validity of a simplified Vs30-equivalent homogeneous medium", *Soil Dyn. Earthq. Eng.*, **131**, 106062. https://doi.org/10.1016/j.soildyn.2020. 106062.

Banerjee, S., Goh, S.H. and Lee, F.H. (2014), "Earthquake-induced bending moment in fixed-head piles in soft clay", *Géotechnique*, **64**(6), 431-446. https://doi.org/10.1680/geot.12.P.195.

Bardet, J.P., Ichii, K. and Lin, C.H. (2000), "EERA: A computer program for equivalent-linear earthquake site response analyses of layered soil deposits", *Research Report*; Department of Civil Engineering, University of Southern California, Los Angeles, CA, USA.

Bouckovalas, G. and Chaloulos, Y. (2014), "Kinematic interaction of piles in laterally spreading ground", *Bull. Earthq. Eng.*, **12**, 1221-1237. https://doi.org/10.1007/s10518-013-9553-1.

Boulanger, R.W., Curras, C.J., Kutter, B.L., Wilson, D.W. and Abghari, A. (1999), "Seismic soil-pile-structure interaction experiments and analyses", *J. Geotech. Geoenviron. Eng.*, **125**(9), 750-759. https://doi.org/10.1061/(ASCE)1090-0241(1999)125:9 (750).

Castelli, F. and Maugeri, M. (2009), "Simplified approach for the seismic response of a pile foundation", *J. Geotech. Geoenviron. Eng.*, **135**(10), 1440-1451. https://doi.org/10.1061/(ASCE)GT. 1943-5606.0000107.

CEN/TC 250 (2003), Eurocode 8: Design of Structures for Earthquake Resistance – Part 5: Foundations, Retaining Structures and Geotechnical Aspects, *European Committee for Standardization*; Brussels, Belgium.

Chen, Z., Li, C. and Zhao, Y. (2024), "Research Progress of Physical Model Test on Slope Reinforcement with Slide-resistant Piles", *Henan Water Resour. South-to-North Water Divers.*, **53**(11), 64-67. http://doi.org/10.12677/hjce.2024.1312243.

Chidichimo, A., Cairo, R., Dente, G., Taylor, C.A. and Maiorano, R.M.S. (2014), "1-g experimental investigation of bi-layer soil response and kinematic pile bending", *Soil Dyn. Earthq. Eng.*, **67**, 219-232. https://doi.org/10.1016/j.soildyn.2014.07.008.

De Sanctis, L., Maiorano, R.M.S. and Aversa, S. (2010), "A method for assessing kinematic bending moments at the pile head", *Earthq. Eng. Struct. Dyn.*, **39**(10), 1133-1154. https://doi.org/10.1002/ eqe.996.

Dezi, F. and Poulos, H.G. (2017), "Kinematic bending moments in square pile groups", *Int. J. Geomech.*, **17**(3), 04016066. https://doi.org/10.1061/(ASCE)GM.1943-5622.0000747.

Dezi, F., Carbonari, S. and Leoni, G. (2010), "Kinematic bending moments in pile foundations", *Soil Dyn. Earthq. Eng.*, **30**(3), 119-132. https://doi.org/10.1016/j.soildyn.2009.10.001.

Di Laora, R. (2023), "Kinematic bending of piles in made ground", *Géotechnique,* **74**(13), 1536-1547. https://doi.org/10.1680/jgeot. 22.00106.

Di Laora, R. and Rovithis, E. (2015), "Kinematic bending of fixed-head piles in nonhomogeneous soil", *J. Geotech. Geoenviron. Eng.*, **141**(4), 04014126. https://doi.org/10.1061/(ASCE)GT.1943-5606. 0001071.

Di Laora, R., Mylonakis, G. and Mandolini, A. (2013), "Pile-head kinematic bending in layered soil", *Earthq. Eng. Struct. D.*, **42**(3), 319-337. https://doi.org/10.1002/eqe.2201.

Dobry, R. and O'Rourke, M.J. (1983), "Discussion of 'Seismic response of end-bearing piles' by Raul Flores-Berrones and Robert V. Whitman (April, 1982)", *J. Geotech. Eng.*, **109**(5), 778-781. https://doi.org/10.1061/(ASCE)0733-9410(1983)109:5(778).

Dutta, S.C. and Roy, R. (2002), "A critical review on idealization and modeling for interaction among soil–foundation–structure system", *Comput. Struct.*, **80**(20-21), 1579-1594. https://doi.org/10.1016/S0045-7949(02)00115-3.

Elahi, H., Moradi, M., Poulos, H.G. and Ghalandarzadeh, A. (2010), "Pseudostatic approach for seismic analysis of pile group", *Comput. Geotech.*, **37**(1-2), 25-39. https://doi.org/10.1016/j.compgeo.2009. 07.001.

Fatahi, B., Basack, S., Ryan, P., Huang, W. and Khabbaz, H. (2014), "Performance of laterally loaded piles considering soil and interface parameters", *Geomech. Eng.*, **7**(5), 495-524. https://doi.org/10. 12989/gae.2014.7.5.495.

Garala, T.K. and Madabhushi, G.S.P. (2021), "Influence of phase difference between kinematic and inertial loads on seismic behaviour of pile foundations in layered soils", *Can. Geotech. J.*, **58**(7), 1005-1022. https://doi.org/10.1139/cgj-2019-0547.

Hokmabadi, A.S., Fatahi, B. and Samali, B. (2014), "Assessment of soil–pile–structure interaction influencing seismic response of mid-rise buildings sitting on floating pile foundations", *Comput. Geotech.*, **55**, 172-186. https://doi.org/10.1016/j.compgeo.2013.08. 011.

Huded, P.M. and Dash, S.R. (2024), "Pile foundation in alternate layered liquefiable and non-liquefiable soil deposits subjected to earthquake loading", *Earthq. Eng. Eng. Vib.*, **23**(2), 359-376. https://doi.org/10.1007/s11803-024-2241-0.

Hussien, M.N., Karray, M., Tobita, T., Iai, S. and Ksibi, A. (2015), "Kinematic and inertial forces in pile foundations under seismic loading", *Comput. Geotech.*, **69**, 166-181. https://doi.org/10.1016/ j.compgeo.2015.05.011.

Itasca (1997), "Fast Lagrangian analysis of continua in 3-dimensions, version 3.0", *Research Report*; Itasca Consulting Group, Minneapolis, MN, USA.

Kagawa, T., Sato, M., Minowa, C., Abe, A. and Tazoh, T. (2004), "Centrifuge simulations of large-scale shaking table tests: case studies", *J. Geotech. Geoenviron. Eng.*, **130**(7), 663-672. https://doi. org/10.1061/(ASCE)1090-0241(2004)130:7(663).

Ke, W. and Zhang, C. (2017), "A closed-form solution for kinematic bending of end-bearing piles", *Soil Dyn. Earthq. Eng.*, **103**, 15-20. https://doi.org/10.1016/j.soildyn.2017.03.009.

Liyanapathirana, D.S. and Poulos, H.G. (2005), "Pseudostatic approach for seismic analysis of piles in liquefying soil", *J. Geotech. Geoenviron. Eng.*, **131**(12), 1480-1487. https://doi.org/10.1061/ (ASCE)1090-0241(2005)131:12(1480).

Luo, R., Yang, M. and Li, W. (2021), "Assessments of kinematic bending moment at pile head in seismic area", *J. Earthq. Eng.*, **25**(5), 970-991. https://doi.org-/10.1080/13632469.2018.1550024.

Maiorano, R.M.S., de Sanctis, L., Aversa, S. and Mandolini, A. (2009), "Kinematic response analysis of piled foundations under seismic excitation", *Can. Geotech. J.*, **46**(5), 571-584. https://doi.org/10.1139/T09-004.

Mánica, M.A., Ovando-Shelley, E. and Botero Jaramillo, E. (2016), "Numerical study of the seismic behavior of rigid inclusions in soft Mexico City clay", *J. Earthq. Eng.*, **20**(3), 447-475. https://doi.org/ 10.1080/13632469.2015.1085462.

Martinelli, M., Burghignoli, A. and Callisto, L. (2016), "Dynamic response of a pile embedded into a layered soil", *Soil Dyn.*

Earthq. Eng., **87**, 16-28. https://doi.org/10.1016/j.soildyn.2016.03.021.

Meymand, P.J. (1998), "Shaking table scale model tests of nonlinear soil-pile-superstructure interaction in soft clay", Ph.D. Dissertation, University of California, Berkeley, CA, USA.

Misirlis, P., Anthi, M., Gerolymos, N. and Vintzileou, E. (2019), "Pile–soil kinematic interaction considering soil nonlinearity and group effects", *Earthquake Geotechnical Engineering for Protection and Development of Environment and Constructions*, CRC Press, Boca Raton, FL, USA.

Mylonakis, G. (2001), "Simplified model for seismic pile bending at soil layer interfaces", *Soils Found.*, **41**(4), 47-58. https://doi.org/ 10.3208/sandf.41.4_47.

Nikolaou, S., Mylonakis, G., Gazetas, G. and Tazoh, T. (2001), "Kinematic pile bending during earthquakes: Analysis and field measurements", *Géotechnique*, **51**(5), 425-440. https://doi.org/10.1680/geot.2001.51.5.425.

Seed, H.B. and Idriss, I.M. (1982), Ground Motions and Soil Liquefaction During Earthquakes, *Earthquake Engineering* Research Institute, Berkeley, CA, USA.

Sica, S., Mylonakis, G. and Simonelli, A.L. (2007), "Kinematic bending of piles: analysis vs. code provisions", *Proceedings of the 4th International Conference on Earthquake Geotechnical Engineering*, Thessaloniki, Greece, June.

Sica, S., Mylonakis, G. and Simonelli, A.L. (2011), "Transient kinematic pile bending in two-layer soil", *Soil Dyn. Earthq. Eng.*, **31**(7), 891-905. https://doi.org/10.1016/j.soildyn.2011.02.001.

Spyrakos, C.C., Maniatakis, C.A. and Koutromanos, I.A. (2009), "Soil–structure interaction effects on base-isolated buildings founded on soil stratum", *Eng. Struct.*, **31**(3), 729-737. https://doi.org/10.1016/j.engstruct.2008.10.012.

Tott-Buswell, J., Garala, T.K., Prendergast, L.J. and Madabhushi, G.S.P. (2022), "Seismic response of piles in layered soils: Performance of pseudostatic Winkler models against centrifuge data", *Soil Dyn. Earthq. Eng.*, **153**, 107110. https://doi.org/10.1016 /j.soildyn.2021.107110.

Vignesh, R. and Muttharam, M. (2023), "Seismic response of pile-raft foundations of a building on layered soil-based design in South India", *J. Geol. Soc. India*, **99**(4), 466-472. https://doi.org/ 10.1007/s12594-023-2334-9.

Zhang, L., Goh, S.H. and Liu, H. (2017), "Seismic response of pile-raft-clay system subjected to a long-duration earthquake: centrifuge test and finite element analysis", *Soil Dyn. Earthq. Eng.*, **92**, 488-502. https://doi.org/10.1016/j.soildyn.2016.10.018

Zhang, N., Shen, F., Dai, D., Yang, W. and Mylonakis, G. (2025), "Kinematic response of large diameter floating pipe piles under vertical S-wave loading", *Acta Geotech.*, 1-17. https://doi.org/10.1007/s11440-025-02532-y.

Zhang, S., Xu, Z. and Deng, C. (2022), "Kinematic responses of a pipe pile embedded in a poroelastic soil to seismic P waves", *Acta Geotech.*, **17**(12), 5533-5556. https://doi.org/10.1007/s11440-022-01517-5.

Zheng, C., Mylonakis, G., Kouretzis, G. and Andrianopoulos, K.I. (2022), "Kinematic seismic response of end-bearing piles to S-waves", *Soil Dyn. Earthq. Eng.*, **163**, 107547. https://doi.org/10.1016/j.soildyn.2022.107547.

CC

Appendix A. List of symbols

$a_{max,S}$: maximum acceleration at the soil surface
d: pile diameter
E_p: pile elastic modulus
E_1: elastic modulus of upper layer
F: dimensionless function of the ratio of the shear moduli of the two layers
G_1: shear modulus of upper layer
G_2: shear modulus of lower layer
H_1: thickness of upper layer
H_2: thickness of lower layer
I_p: pile inertia moment
k_1: soil–spring stiffness
L: pile length
r: pile radius
V_{S1}: shear wave velocity of upper layer
V_{S2}: shear wave velocity of lower layer
φ: amplification factor accounting for excitation frequency, typically less than 1.25, 1.0 for preliminary design
φ^*: amplification factor, 1.39 and 1.30 for resonant and non-resonant conditions, respectively
β: coefficient, 0.075 and 0.069 for resonant and non-resonant conditions, respectively
$\varepsilon_{p:}$ bending strain at the outer fiber of the pile cross section
v: Poisson's ratio of soil
γ_1: maximum soil shear strain at the interface
γ_1^*: maximum soil shear strain at the interface, calculated by EERA
r_d: depth factor
ρ_1: density of the upper layer
τ_c: characteristic shear stress at the interface
τ_c^*: characteristic shear stress at the interface, calculated by EERA
z: depth of interface
s: pile spacing
B: raft width
K: bulk modulus
z_{min}: the smallest width of an adjoining zone in the normal direction, 1m in this study.
M: kinematic bending moments
M_p: predicted kinematic bending moment
M_c: kinematic bending moment obtained from numerical simulation
ξ_{min}: the critical damping ratio
f_{min}: central frequency
E_R: Young modulus
v_R: Poisson's ratio
f_p: the seismic peak frequency
k: the normal and shear stiffness

Appendix B.

Appendix Table 1 Analysis cases of double-layered ground

No.	V_{S1} (m/s)	V_{S2} (m/s)	H_1 (m)	H_2 (m)	d (m)	D (%)	ρ (kg/m^3)	L (m)	v
D1-1					0.6	2			
D1-2					0.6	5			
D1-3	100	400	15	15	0.6	8			
D1-4					0.3	10			
D1-5					0.7	10			
D1-6					1	10			
D2-1			5	25					
D2-2	200	400	10	20	0.6	10			
D2-3			15	15					
D3-1			5	25					
D3-2	100	200	10	20	0.6	10			
D3-3			15	15					
D4-1	60								
D4-2	70	400	10	20	0.3	10	1940	20	0.4
D4-3	80								
D4-4	90								
D5-1	60								
D5-2	70	400	10	20	0.5	10			
D5-3	80								
D5-4	90								
D6-1	60								
D6-2	70	400	10	20	0.6	10			
D6-3	80								
D6-4	90								
D7-1	60								
D7-2	70	400	10	20	0.7	10			
D7-3	80								
D7-4	90								

Appendix Table 2 Analysis cases of triple-layered ground

No.	$VS1$ (m/s)	$VS2$ (m/s)	$VS3$ (m/s)	$H1$ (m)	$H2$ (m)	$H3$ (m)	d (m)	D (%)	ρ (kg/m3)	L (m)	v
T1-1				2		18					
T1-2	200	100	400	5		15					
T1-3				8		12					
T1-4				10		10	0.6				
T2-1				2		18					
T2-2	100	50	400	5		15					
T2-3				8		12					
T2-4				10		10					
T3-1				2		18					
T3-2	200	100	400	5		15	1				
T3-3				8		12					
T3-4				10		10					
T4-1				2		18					
T4-2	130	100	400	5	10	15		10	1940	20	0.4
T4-3				8		12					
T4-4				10		10					
T5-1				2		18					
T5-2	150	100	400	5		15					
T5-3				8		12					
T5-4				10		10	0.6				
T6-1				2		18					
T6-2	180	100	400	5		15					
T6-3				8		12					
T6-4				10		10					
T7-1				2		18					
T7-2	300	100	400	5		15					
T7-3				8		12					
T7-4				10		10					